STRUCTURAL BEHAVIOUR AND ROBUSTNESS ASSESSMENT OF AN INFRACORE® INSIDE BRIDGE DECK SPECIMEN SUBJECTED TO STATIC AND DYNAMIC LOCAL LOADING

Wouter De Corte[1], Arne Jansseune[2], Wim Van Paepegem[3] and Jan Peeters[4]

[1] Structural Engineering Department, Faculty of Engineering and Architecture, Ghent University, Valentin Vaerwyckweg 1, 9000 Ghent, Belgium, wouter.decorte@ugent.be, www.ugent.be/ea/structural-engineering/
[2] Structural Engineering Department, Faculty of Engineering and Architecture, Ghent University, Valentin Vaerwyckweg 1, 9000 Ghent, Belgium, arne.jansseune@ugent.be, www.ugent.be/ea/structural-engineering/
[3] Department of Materials, Textiles and Chemical Engineering, Faculty of Engineering and Architecture, Ghent University, Technologiepark Zwijnaarde 903, 9052 Zwijnaarde, wim.vanpaepegem@ugent.be, www.ugent.be/ea/match/
[4] InfraCore Company, Oostdijk 25, 3077 CP Rotterdam, the Netherlands, peeters@infracore-company.com, http://www.fibercore-europe.com/

Keywords: Bridge deck, Robustness, InfraCore® Inside, Fatigue, Web buckling, Finite element

ABSTRACT

The paper presents static and dynamic test results for specimens taken from an InfraCore® Inside bridge deck panel subjected to traffic loads. This InfraCore® technology is developed for the construction of a robust FRP panel that is applicable for highly loaded structures. In general, the drawback in traditional FRP sandwich structures has always been debonding of skin and core. Such debonding problem may occur after impact, followed by fatigue loading. Through the use of the InfraCore® technology, such debonding is no longer possible, as multiple overlapping Z-shaped and two-flanged web structures are alternated with polyurethane foam cores acting as non-structural permanent formwork. Consequently, the fibres in the upper and lower skins as well as in the vertical webs run in all directions, especially in the connection between them, rendering a resin-dominated crack propagation impossible. In order to determine the effectiveness under controlled circumstances, a number of test samples were cut from an InfraCore® bridge deck and subjected to static loading and fatigue loading cycles with induced damage. After determination of the elastic properties, a number of three point bending tests are carried out to assess the robustness of the system, with prior damage, introduced as a horizontal 1mm wide and 25mm long gap in the rib to skin connection at the point of calculated maximum principal stress in the 3PBT. The results indicate that after 1.000.000 load cycles of 60 kN no observable crack growth was noted, even after damage introduction. In a second test with prior damage, the fatigue load was increased from 60 kN in 5 kN steps every 10.000 cycles. Again, no observable damage was detected until buckling of the web directly underneath the load at 95 kN after 61.395 load cycles occurred. Both results corroborate the robustness claim of the InfraCore® Inside technology.

1 INTRODUCTION

InfraCore® is a patented [1-2] technology specifically designed for the construction of robust fibre reinforced panels for highly loaded applications [3]. It distinguishes itself from all other existing technologies in the way it deals with debonding of skin and core, especially after initial impact damage. This debonding has always been the Achilles heel of many regular FRP structures, and occurs mainly after impact, followed by fatigue (See Figure 1). In a classic skin-core-skin sandwich element, initial damage to the upper flange and to the core material will initiate local debonding. Any following fatigue loading will result in further and uncontained debonding, and eventually in complete structural failure. This failure mechanism indicates a lack of robustness of the structural concept, and has to be avoided [4]. Impact, followed by fatigue is a typical scenario for civil applications (e.g. bridge decks

and lock gates) limiting the use of classical sandwiches. Although classical sandwiches are uncommon in civil applications, the described failure pattern will also be created when the panel is built up of multiple parallel fibre reinforced beams, even when additional flange layers are added. In any case, uncontrolled resin dominated crack paths can develop after initial local damage, proving that all these concepts lack inherent robustness desired in civil structures [5][6].

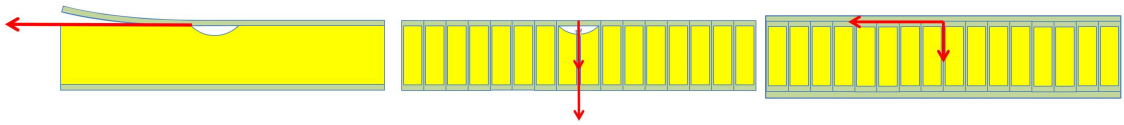

Figure 1: Uncontrolled debonding after local damage.

To overcome these problems, a unique structure has been developed. This sandwich-like structure prevents skin-core debonding by skin fibres protruding in the webs and vice versa (See Figure 2). To achieve this, the basic shape of the fabric layout is a Z-profile, providing fibre continuity between skin and webs. In this way, uncontrolled resin dominated cracking (Figure 1) is avoided. The polyurethane core material mainly serves as a spacer during manufacturing but also provides some buckling restraint to the webs.

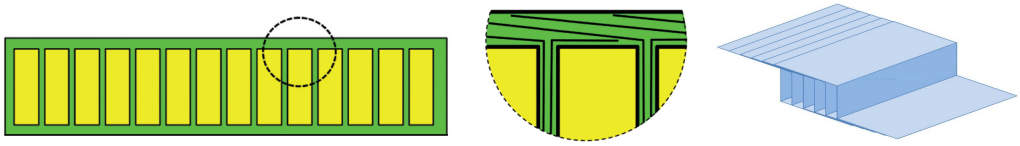

Figure 2: Principle of InfraCore® Inside.

Although the fibre lay-up can be tailored according to specific situations, a typical Z-profile composition might be (See Figure 3) : one Z-shaped layer of 45/-45°(50%/50%) fabric, one additional flat UD-0°-layer in the flanges, and one additional flat UD-90°-layer in the web. This Z-shaped fabric building block is stacked with foam core elements in between creating an InfraCore® Inside sandwich panel.

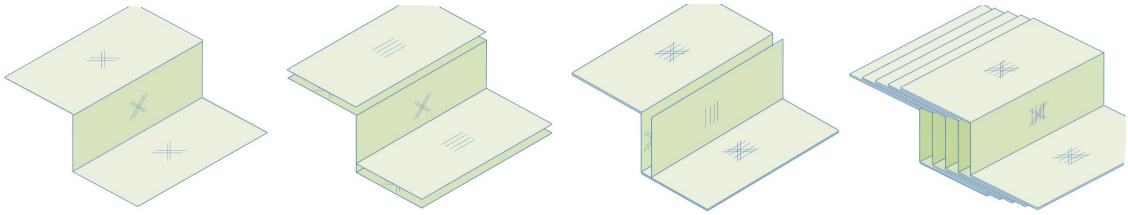

Figure 3: InfraCore® Inside: fabric stacking sequence.

Although he foam cores serve mainly during the production process, other functions can be attributed as well. For road bridges requiring resistance to concentrated wheel loads additional vertical corrugated fabric layers may be introduced inside the foam cores (See Figure 4).

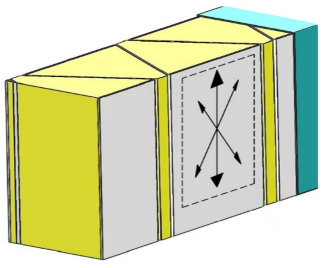

Figure 4: Additional corrugated reinforcement inside the core elements.

These thin corrugated ribs not only provide lateral buckling resistance to the webs, but also increase the overall transverse shear stiffness of the panel, contributing to load spreading. The laminate typically consists of a 90/45/-45°(50%/25%/25%) fabric.

In order to determine the effectiveness of flawed specimens under controlled circumstances, a number of test samples were cut from an InfraCore® Inside bridge deck and subjected to static loading and fatigue loading cycles with induced damage. In the first part of this paper, the three point bending (3PBT) test setup is presented, and the experimental results are reported. In the second part of this paper, the test results are related to numerical results from a finite element calculation using Abaqus as numerical tool. Finally, conclusions are drawn.

2 TEST SETUP

The three point bending setup (See Figure 5) consists of a rigid support beam on which two roller supports are mounted creating a 365mm span, the test specimen, a neoprene load surface of 50mm (Specimen 1) and 100mm (Specimen 2) lengthwise, and a rigid load introduction block of equal length. The dimensions of the test samples are for specimen 1: 415mm (L) x 111mm (W) x 169mm (H) and for specimen 2: 416mm (L) x 111mm (W) x 169mm (H). The load is generated by a hydraulic actuator with a maximum capacity of 250kN.

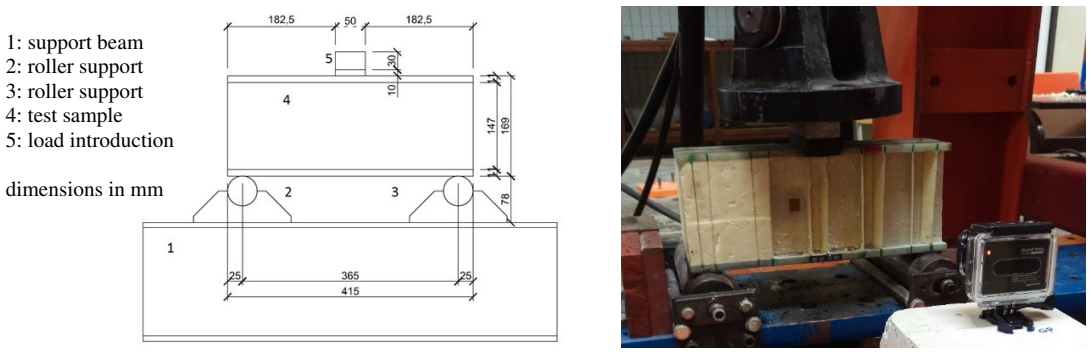

Figure 5: Test setup (for 50mm load width).

The test specimens are cut from a larger InfraCore® bridge deck sample (See Figure 2). The top flange has a thickness of 11mm and 2 longitudinal webs of 8mm thickness are present in the samples. The basic properties of the flange and web laminates are presented in Table 1.

	Engineering constant		Value
skin	E_0	[GPa]	27,738
skin	$E_{90°}$	[GPa]	13,550
skin	$\nu_{0/90°}$	–	0,135
skin	$G_{0/90°}$	[GPa]	2,401
web	E_0	[GPa]	12,267
web	$E_{90°}$	[GPa]	16,372
web	$\nu_{0/90°}$	–	0,158
web	$G_{0/90°}$	[GPa]	3,003
foam	E	[GPa]	0,01
foam	ν	–	0,32

Table 1: Basic mechanical properties of flange and web laminates.

In both samples a flaw was introduced as a 25mm long longitudinal crack in a web (See Figure 6), vertically directly under the top flange, and horizontally a the location of maximum shear transfer between flange and web (i.e. between 100 and 125mm) from the supports. Specimen 1 was tested in

3PBT with a load width of 50mm and subjected to 1.000.000 load cycles at 3Hz of 60 kN (5 – 65 kN), after which it was loaded up to failure. Specimen 2 was tested in 3PBT with a load width of 100mm and subjected to successive batches of 10.000 load cycles at 3 Hz of increasing size, starting with 60 kN (5-65 kN), and increasing by 5 kN after each batch. No specimens failed in fatigue, but rather due to web buckling, followed by interlaminar failure of the top flange. As this implicates that the specimens may retain some of their strength and stiffness, the samples were rotated over 180° around their longitudinal axis and subjected to a static test up to failure to assess their residual strength.

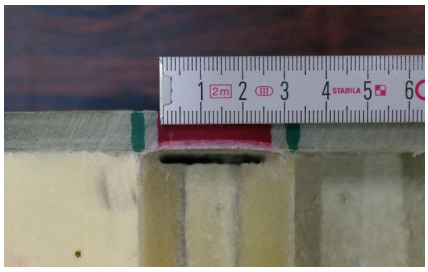

Figure 6: longitudinal flaw introduction in web (25mm).

3 TEST RESULTS

3.1 Specimen 1

A first series of tests was conducted on specimen 1. In this series the load width (in the span direction) is 50mm. Based on finite element analysis (See paragraph 4) a maximum shear induced principal tensile stress at the flaw edge was found as 2,18 MPa per kN. For a 60 kN load this amounts to 130,8 MPa. The Dutch recommendation CUR96 [7] for FRP in civil applications relates the number of cycles up to failure for this particular material to the applied stress as :

$$N_f = \left(\frac{\sigma_{amp} \cdot \gamma_m \cdot \gamma_c}{\sigma_{Rk}}\right)^{-k} \quad (1)$$

In an unfactored test situation (γ_m=1;γ_c=1), and with k=9 (glass – polyester) and σ_{Rk} = 497 MPa (static tensile strength) the number of cycles up to failure should exceed 165.096 cycles. Specimen 1 was subjected to 1.000.000 load cycles of 60 kN (5kN – 65kN) in the 3PBT setup described in paragraph 2. No indication of crack propagation at the flaw was found, hereby exceeding the expected number of cycles at least 6 times. Evidently, it should be noted that this comparison is based on a calculated and not experimentally verified stress, that cannot be calculated nominally. After this, the specimen was subjected to a monotonic load increase up to 90kN at which the specimen failed due to buckling of the longitudinal webs followed by interlaminar failure of the laminate in the top flange (See Figure 7). This failure corresponds to an average vertical pressure on the webs of 112,5 MPa directly under the load. It should be noted that given that the specimen was cut from a larger part, the contribution of the corrugated web stiffeners, interrupted by the saw cut (See Figure 7) is negligible. In a continuous specimen, the resistance to direct load introduction is probably higher.

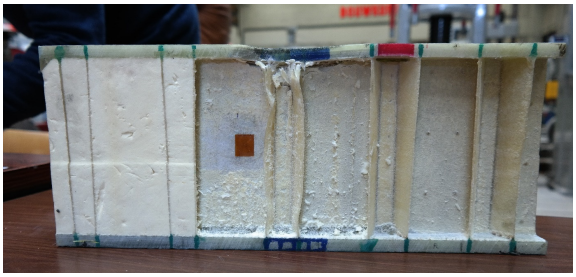

Figure 7: Specimen 1 after failure.

After completion of the test, it was noted that although the specimen failed, it did not collapse, and maintained integrity. To assess how much integrity was left, the specimen was rotated top to bottom

(i.e. 180° rotation around the longitudinal axis) and subjected to static testing up to failure. Figure 8 shows the vertical deformation of the test sample at midspan. Initially, the specimen shows substantial deformation increases, but these stabilize after roughly 10 kN and then monotonically increase with 0,0340 mm/kN up to failure at 133 kN, again due to buckling of the web under the load (See Figure 8), but remarkably at a much higher total load. This corresponds to an average vertical pressure on the webs of 166,25 MPa directly under the load. Apparently, the fatigue loading has indeed decreased the web buckling resistance to some extent. Nevertheless, in service conditions no actual fatigue load on a bridge is limited a surface as small as the one used in the test setup, so this phenomenon is not to be feared. The remaining stiffness of 0,0340 mm/kN corresponds very well to the initial stiffness of the specimen, not measured during the fatigue test on this specimen but found from previous static testing on similar specimens with equal laminate specifications.

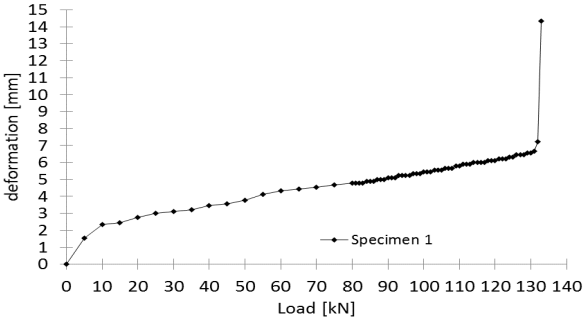

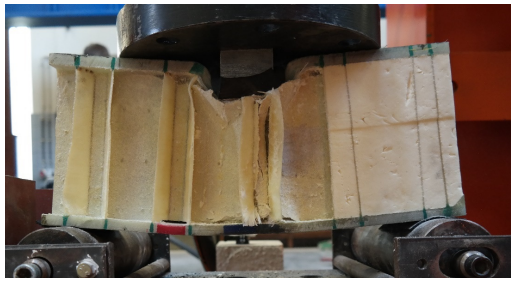

Figure 8: Vertical deformation (midspan) of failed specimen top down in 3PBT / failure mode.

3.2 Specimen 2

A second series of tests was conducted on specimen 2. In this series, and based on the failure phenomenon from specimen 1, the load width (in the span direction) is doubled to 100mm to reduce the risk of premature failure due to web buckling. Based on finite element analysis (See paragraph 4) a maximum shear induced principal tensile stress at the flaw edge was found of 2,33 MPa per kN. For a 60 kN load this amounts to 139,8 MPa. By application of Eq. 1, the number of cycles up to failure should exceed 90707 cycles. However, given the significant underestimation of the expected number of cycles of specimen 1, it was chosen to increase the load in steps of 5 kN after each batch of 10.000 cycles (i.e. 5-65 kN / 5-70 kN / etc). When applying a Miner's rule approach of cumulative damage, the damage level of each consecutive batch is almost double that of the previous one (See Figure 9).

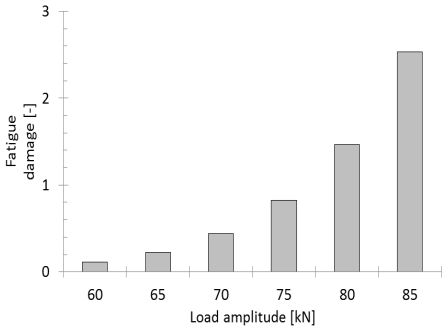

Figure 9: Fatigue damage per batch of 10.000 cycles (Specimen 2).

Specimen 2 was subjected to 10.000 load cycles of 60/65/70/75/80/85 kN in the 3PBT setup described in paragraph 2, totalling 60.000 cycles and a cumulative damage of 5,6 (based on calculated stresses), far exceeding the expected number of cycles. Again, no indication of crack propagation at the flaw was found. After this, the subject was subjected to a 90 kN cycle (5-95 kN) for which the specimen failed after only 1.395 cycles, again due to buckling of the longitudinal webs followed by failure of the laminate in the top flange (See Figure 10). This failure corresponds to an average vertical pressure on the webs of 59,37 MPa directly under the load. This value is considerably smaller than in

specimen 1, but in fact the failure phenomenon was observed to be asymmetric, with essentially one web failing. This can be attributed to a transversely slightly asymmetric location of the webs in the test specimen. It should again be noted that as the specimen was cut from a larger part, the contribution of the corrugated web stiffeners, interrupted by the saw cut (See Figure 10) is negligible. Due to both reasons, the resistance to direct load introduction is certainly higher in a continuous specimen.

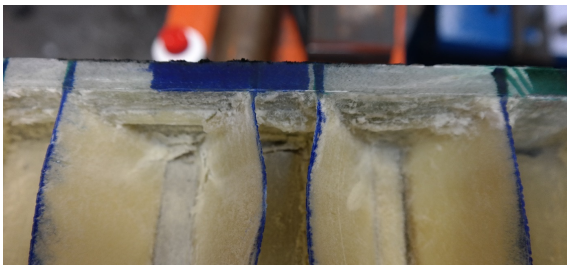

Figure 10: Specimen 2 after failure (detail).

After completion of the test, it was again noted that although the specimen failed, it did not collapse, and maintained integrity. To assess how much integrity was left, the specimen was rotated top to bottom (i.e. 180° rotation around the longitudinal axis) and subjected to static testing up to failure. Figure 11 shows the vertical deformation of the test sample at midspan. Initially, the specimen shows substantial deformation increases, but these stabilize after roughly 10 kN and then monotonically increase with 0,0308 mm/kN up to failure at 118 kN. In this case failure initiated at the left support initiating delamination in the webs. The fact that the web did not fail at midspan again indicates that the fatigue loading has probably also here decreased the web buckling resistance to some extent. In service conditions this phenomenon is not to be feared. The remaining stiffness of 0,0308 mm/kN is slightly smaller compared to the value of Specimen 1 corresponding to the wider load area..

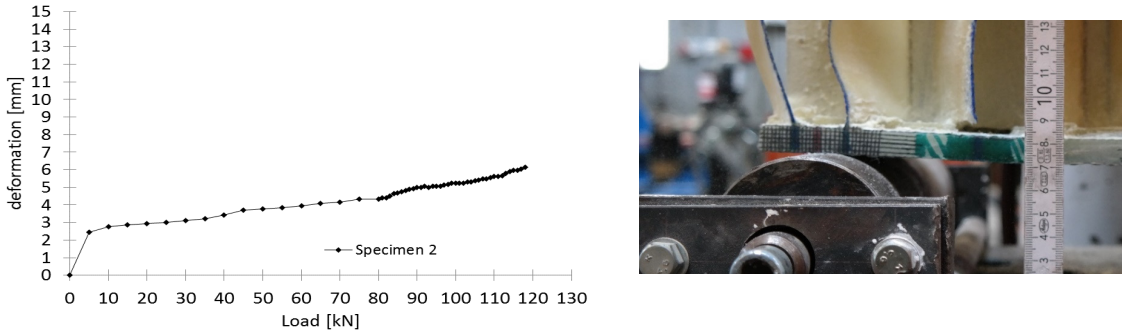

Figure 11: Vertical deformation (midspan) of failed specimen top down in 3PBT / failure mode.

4 FINITE ELEMENT MODEL AND RESULTS

In order to assess the values for the load amplitude level in the static and fatigue tests of paragraph 2, a numerical model was generated with the finite element software Abaqus [8]. Figure 12 displays the numerical model. A combination of linear hexahedral elements (C3D8) and linear wedge elements (C3D6) are used, totaling 670.057 elements. For the stress assessment at the flaw, the number of elements is locally increased totaling 4.492.712 for the most detailed model. Linear elastic material properties are attributed in line with Table 1, and a load of 1 kN is applied to the steel loading surface. In Figure 13 the vertical deflection are visualized for both specimens proving good accordance with the vertical deflection values in the robustness tests mentioned in paragraph 3. Figure 14 shows the main stress components (CSYS : global) per kN applied load in the test specimen. General longitudinal bending, local transverse bending and vertical stresses in the webs are clearly visible. Finally, Figure 15 shows the shear induced longitudinal stresses on the bottom side of the top flange, calculated for specimen 2 in the most detailed model as 2,33 MPa per kN (See paragraph 3). Although the model is already quite elaborate, it could be further improved as it does not include geometric non-

linearities, buckling analysis, cohesive behavior etc. However, the results are already much more detailed than found from analytical orthotropic plate theory as commonly used in bridge deck analysis, especially in the vicinity of loads, supports, and flaws.

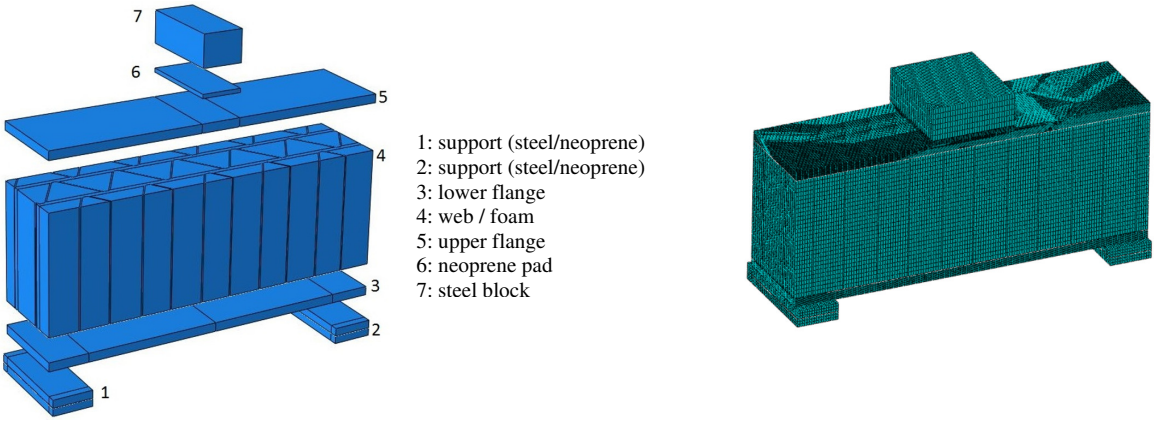

Figure 12: Numerical model (50mm load (left) – 100mm load (right)).

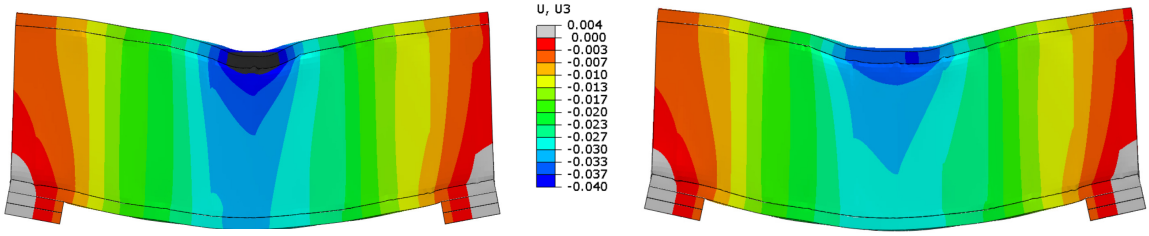

Figure 13: Vertical deflections per kN [mm] (50mm load (left) – 100mm load (right)).

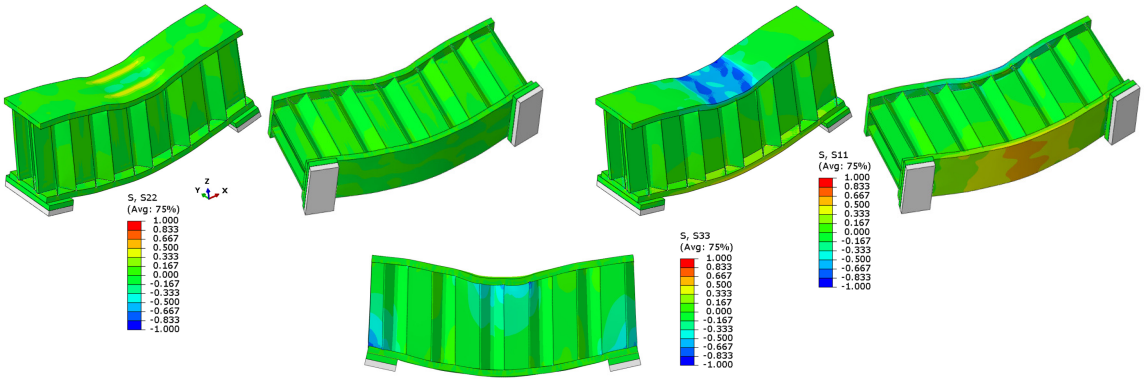

Figure 14: Stresses per kN [MPa] for specimen 2 model (CSYS : Global)

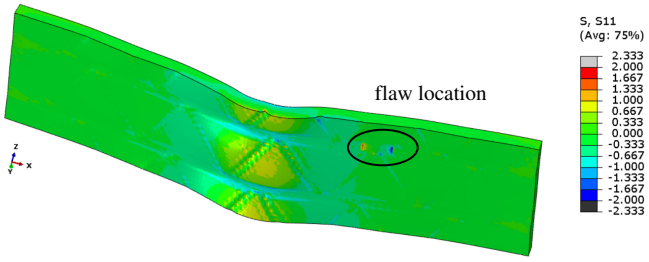

Figure 15: Stresses per kN [MPa] for specimen 2 model (lower side of top flange) (CSYS : Global)

9 CONCLUSIONS

Two InfraCore® Inside test samples cut from a larger bridge deck panel were loaded in fatigue. In each specimen, a 25 mm longitudinal flaw was created between the upper flange and a web. A first specimen was subjected to 1.000.000 load cycles of 60 kN amplitude, after which no observable crack growth was noted. The cumulative damage at this point, as calculated by finite element analysis, exceeded D=6. Statically, the specimen failed at 90 kN, due to web buckling, followed by interlaminar failure of the laminate in the top flange. However, although the specimen failed, it did not collapse, and maintained integrity. In order to assess how much integrity was left, the specimen was rotated top to bottom and subjected to static testing up to failure, and failed only at 133 kN, proving that for an InfraCore® Inside object local damage and even failure does not automatically lead to complete loss of structural integrity, as it would with many other sandwich panel types. A second specimen was subjected to a series of fatigue load batches of 10,000 cycles with increasing amplitude. Very similar conclusions regarding underestimation of fatigue life of the flawed specimen, eventual failure mode and residual strength could be drawn. The results of both small scale tests corroborate to the robustness claim of the InfraCore® technology.

ACKNOWLEDGEMENTS

The authors wish to acknowledge Christof Linke and Tibo Suvée for their contribution in the numerical modelling and the experiments.

REFERENCES

[1] J.H.A. Peeters, Patent WO2010008293, Sandwich panel and method for producing such a panel, FiberCore IP bv, 2009-2010.

[2] J.H.A. Peeters, Patent WO2010059048, Method of producing a panel and a core therefor, FiberCore IP bv, 2009-2010.

[3] M. Veltkamp and J. Peeters, Hybrid Bridge Structure Composed of Fibre Reinforced Polymers and Steel, *Structural Engineering International*, **24(3)**, 2014, pp. 425-427.

[4] European Committee for Standardization, EN 1990: 2002 - Eurocode - Basis of structural design, consolidated version, including A1:2005 and AC:2010, CEN, Brussels, 2015.

[5] L.Wang, L. Weiqing, L. Wan, H. Fang, and D. Hui, Mechanical performance of foam-filled lattice composite panels in four-point bending: Experimental investigation and analytical modeling. *Composites : Part B*, **67**, 2014, pp. 270-279.

[6] D.Y. Moon, G. Zi, D.H. Lee, B.M Kim and & Y.K. Hwang, Fatigue behavior of the foam-filled GFRP bridge deck, *Composites : Part B*, **40**, 2009, pp. 141-148.

[7] CUR, CUR- Aanbeveling 96: Vezelversterkte kunststoffen in civiele draagconstructies, CUR, Delft, 2003 (in Dutch).

[8] ABAQUS 2016, ABAQUS Documentation, Dassault Systèmes, Providence, 2016.